

New AMD3100 derivatives for CXCR4 chemokine receptor targeted molecular imaging studies: synthesis, anti-HIV-1 evaluation and binding affinities †

Sophie Poty ^a, Pauline Désogère ^a, Christine Goze ^{*a}, Frédéric Boschetti ^b, Thomas D'huys ^c, Dominique Schols ^c, Christopher Cawthorne ^d, Stephen J. Archibald ^d, Helmut R. Maëcke ^e and Franck Denat ^{*a}

^aICMUB (UMR CNRS 6302), 9 Av. Alain Savary, BP 47870 21000 Dijon, France. E-mail:

christine.goze@u-bourgogne.fr; franck.denat@u-bourgogne.fr

^bChematech, 9 Av. Alain Savary, BP 47870 21000 Dijon, France

^cRega Institute for Medical Research, KU Leuven, B-3000 Leuven, Belgium

^dPositron Emission Tomography Research Centre, The University of Hull, Cottingham Road, Hull HU67RX, UK

^eUniversitätsklinikum Freiburg, IMSRobert-Koch-Str. 1, Freiburg, D-79106, Germany

Received 26th September 2014 , Accepted 20th January 2015

First published on the web 20th January 2015

CXCR4 is a target of growing interest for the development of new therapeutic drugs and imaging agents as its role in multiple disease states has been demonstrated. AMD3100, a CXCR4 chemokine receptor antagonist that is in current clinical use as a haematopoietic stem cell mobilising drug, has been widely studied for its anti-HIV properties, potential to inhibit metastatic spread of certain cancers and, more recently, its ability to chelate radiometals for nuclear imaging. In this study, AMD3100 is functionalised on the phenyl moiety to investigate the influence of the structural modification on the anti-HIV-1 properties and receptor affinity in competition with anti-CXCR4 monoclonal antibodies and the natural ligand for CXCR4, CXCL12. The effect of complexation of nickel(II) in the cyclam cavities has been investigated. Two amino derivatives were obtained and are suitable intermediates for conjugation reactions to obtain CXCR4 molecular imaging agents. A fluorescent probe (BODIPY) and a precursor for ¹⁸F (positron emitting isotope) radiolabelling were conjugated to validate this route to new CXCR4 imaging agents.

Introduction

The CXCR4 chemokine receptor is a seven transmembrane helix protein, and member of the G-protein-coupled receptor (GPCR) superfamily.¹ It has only one naturally occurring endogenous ligand known as SDF-1 or CXCL12.² Together with its natural ligand, CXCR4 is a central part of the signalling system in the human body that results in a variety of normal physiological responses, such as chemotaxis, cell survival and proliferation, intracellular calcium flux, and gene transcription. However CXCR4 is also involved in the pathogenesis of a wide range of diseases.³ Malignant cells from at least 23 different types of cancer express the chemokine receptor CXCR4 and respond to its ligand CXCL12.⁴ Furthermore, CXCR4 is a co-receptor for T-cell tropic strains of human immunodeficiency virus-1 (HIV-1) and allows fusion and entry of the virus into human white blood cells.⁵ Hence, CXCR4 is a target of growing interest for the development of anti-HIV drugs and in the field of diagnostic oncology. Clinically AMD3100 is used in combination with G-CSF (granulocyte colony stimulating factor) to mobilise haematopoietic stem cells and allow harvesting.

Inhibition of the CXCR4-CXCL12 signalling was investigated as a therapeutic strategy using antagonists of the natural ligand. Several CXCR4-binding agents, including antibodies and peptide-based antagonists have been developed.⁶ In the search for new anti-HIV agents, bicyclam compounds were discovered as CXCR4 antagonists with potent and selective anti-HIV activities.⁷ These molecules consist of two 14-member tetraaza macrocyclic rings, linked either by an aliphatic bridge or an aromatic bridge such as AMD3100. The latter, unlike many other existing HIV drugs that target the virus after it has infected a healthy cell, blocks the virus from entering the cell, inhibiting the replication of both HIV-1 and HIV-2.⁸ AMD3100 binds to the CXCR4 chemokine receptor mainly *via* electrostatic interaction between the positively charged protonated amino nitrogens of the cyclam moieties and the negatively charged carboxylates of the aspartate and glutamate residues of the receptor.⁹ AMD3100 has also been demonstrated to be a ligand for another chemokine receptor, CXCR7. In contrast to its antagonistic effect blocking the CXCR4/CXCL12 interaction, AMD3100 positively modulates CXCL12 effects on binding to CXCR7, it is therefore qualified as an allosteric agonist of CXCR7.¹⁰ AMD3100 was clinically tested as an anti-HIV drug but the trial was discontinued in favour of an orally available CXCR4 antagonist.¹¹ Nevertheless, AMD3100 demonstrated a great potential in hematopoietic stem cell

mobilisation and is now approved by the U.S. Food and Drug Administration for use in non-Hodgkin's lymphoma and multiple myeloma patients.¹²

With the aim of optimising the anti-HIV activity of bis-azamacrocycles, many parameters of AMD3100 have been studied to determine the modifications that can be tolerated whilst maintaining high CXCR4 receptor affinity. Analogues were synthesised either with a different linker, a macrocycle ring size varying from 12 to 16 ring members,¹³ the introduction of one or more heteroatoms in the macrocycle ring or replacement of one amino group by a heteroaromatic, all analogues resulting in a reduced anti-HIV potency (Fig. 1).¹⁴

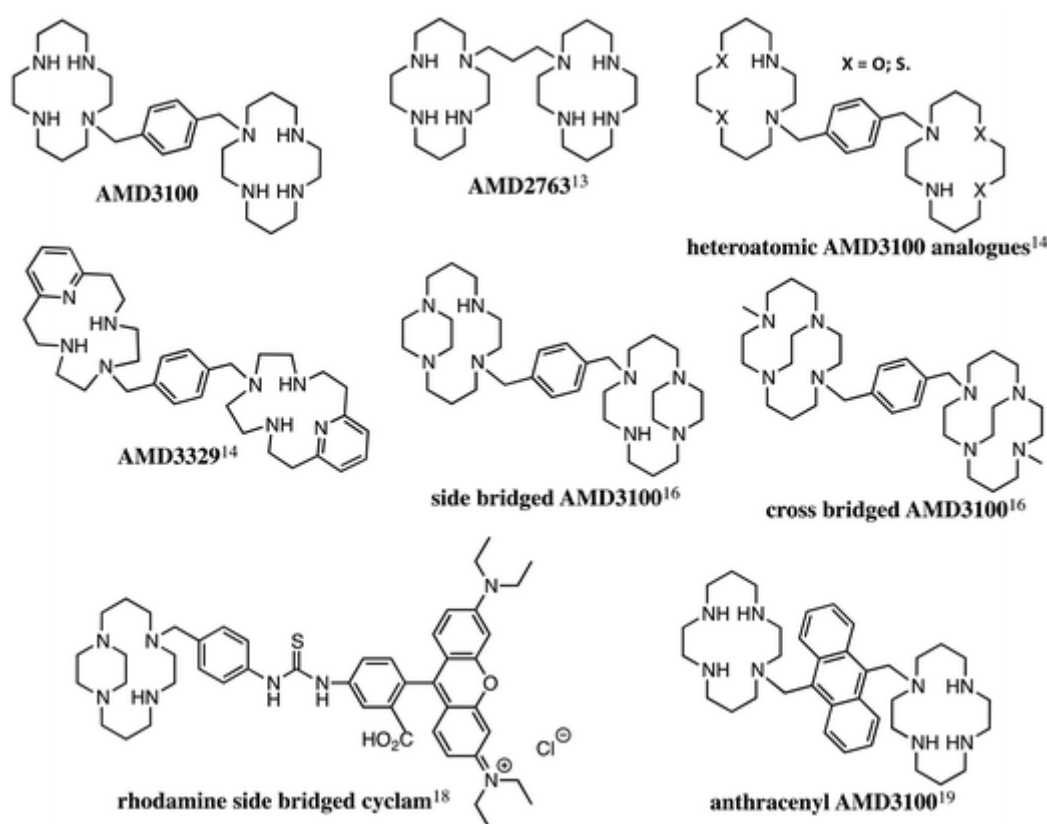


Fig. 1 AMD3100 and derivatives studied for their anti-HIV activities and CXCR4 affinities.

Because of the preorganisation and the flexibility of their macrocyclic framework, macrocyclic polyamines such as cyclam, are known to bind to metal ions and form highly stable metal complexes. Complexes of AMD3100 with metal cations were prepared and the incorporation of Zn^{II}, Ni^{II} and Cu^{II} led to the enhancement of the binding affinity to CXCR4 receptor and a higher anti-HIV activity in most cases. The nickel(II) complex of AMD3100 in solution can adopt the folded (*cis*-V) and planar (*trans*-III) configuration, rearranging to

give the *cis*-V compound on binding to the protein aspartate residues.¹⁵ Studies with AMD3100 analogues complexes with configurationally restricted macrocycles, where ethyl bridges link adjacent and non-adjacent nitrogen atoms to give respectively side and cross bridged cyclams, demonstrated that the rigidification of the cyclic scaffold may be a route toward the optimisation of the interactions of the antagonist with the receptor.¹⁶ Additionally, as metal ion incorporation was shown to enhance the affinity of AMD3100 for its receptor, the ligand was used for direct radiolabelling with ⁶²Zn, ⁶⁴Cu, ⁶⁷Ga and ^{99m}Tc, resulting in tracers suitable for positron emission tomography (PET) and single-photon emission computed tomography (SPECT) to image CXCR4 expression in human cancer xenografts in mice.¹⁷

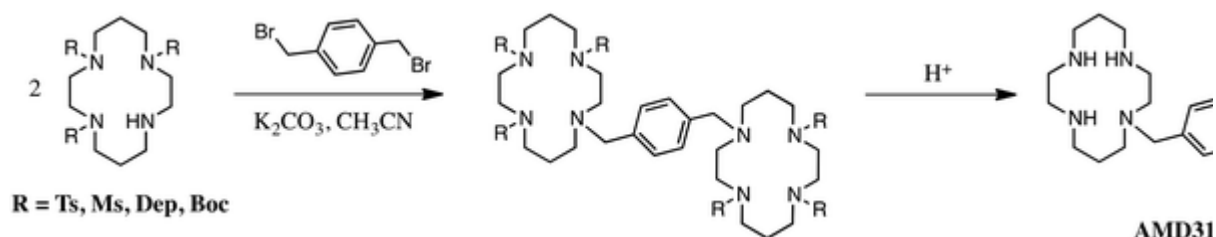
Only two examples of optical CXCR4 imaging agents based on cyclam structures have been studied despite the advantages of optical imaging. A rhodamine conjugated to a reinforced cyclam competes with anti-CXCR4 antibodies during binding competition when labelled with copper(II)¹⁸ and a fluorescent AMD3100 analogue with an anthracenyl moiety used as a spacer shows a significant reduction of the affinity probably due to the lipophilic character of the anthracenyl group.¹⁹

In this study, new CXCR4 antagonists are investigated as potent anti-HIV agents and platforms for conjugation in molecular imaging agent design. The syntheses of new AMD3100 analogues functionalised on the phenyl moiety by an ester or an ethylenediamine moiety are discussed and we report the influence of the functionalisation on the affinity towards the CXCR4 chemokine receptor and antiviral potency against an X4 HIV-1 strain. Metal complex formation with nickel(II) and the influence on the binding and antiviral potency will also be presented. Ni²⁺ was chosen because its incorporation in the biscyclam AMD3100 enhances the binding to the chemokine receptor CXCR4 by 50-fold. This is the highest affinity obtained by incorporation of a transition metal.²² Finally, the functionalisation on the phenyl spacer allowed the introduction of an imaging component, *i.e.* optical probe or PET imaging agent precursor, confirming the versatility of the modified AMD3100 derivatives.

Results and discussion

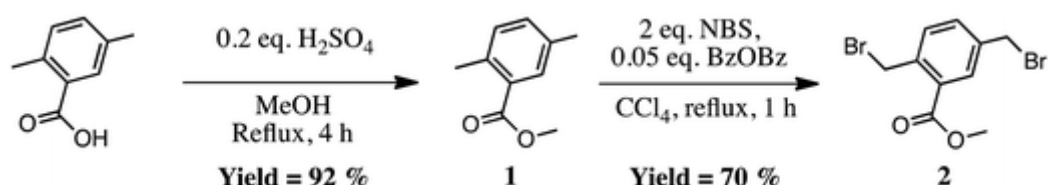
Synthetic procedures

Several synthetic routes to produce AMD3100 are reported in the literature.²⁰ A cyclam ring protected with tosyl, mesityl, diethylphosphoramidate (Dep) or *tert*-butoxycarbonyl (Boc) groups is used as a starting material. Indeed, the best synthetic approach for bridging two macrocyclic units is to use a triprotected tetraazamacrocycle, in order to avoid the formation of polymers. Boc protecting groups were chosen as they can be easily removed by acidic treatment. The reaction of the protected macrocycle with α,α -dibromo-*p*-xylene and the deprotection in acidic conditions give access to AMD3100 in two steps ([Scheme 1](#)).



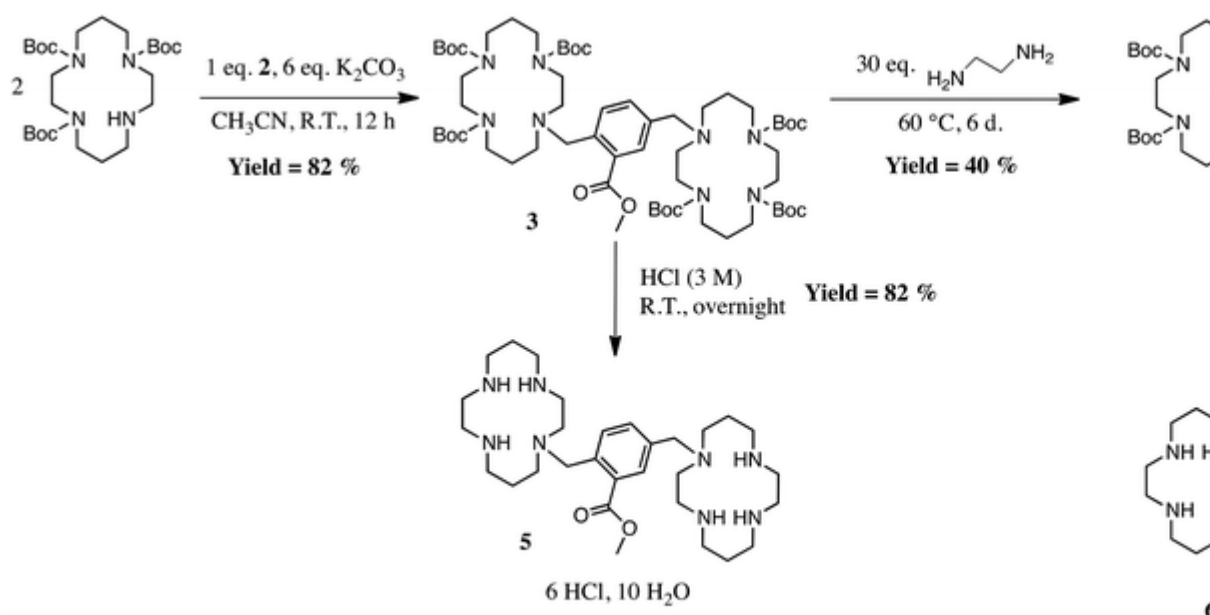
Scheme 1 General synthesis of AMD3100.

To investigate the influence of a functionalisation of the phenyl moiety on AMD3100 properties, we considered the synthesis of a *p*-dibromoxylyl spacer substituted with an ester group. The precursor is obtained in two steps ([Scheme 2](#)) starting from a commercially available product, 2,5-dimethylbenzoic acid.²¹ Esterification with methanol using sulfuric acid as a catalyst yields compound **1** in 92% yield. **2** is then prepared through NBS-based bis-bromination of the aryl methyl groups of **1**.



Scheme 2 Synthesis of a dibromo aromatic spacer bearing an ester group.

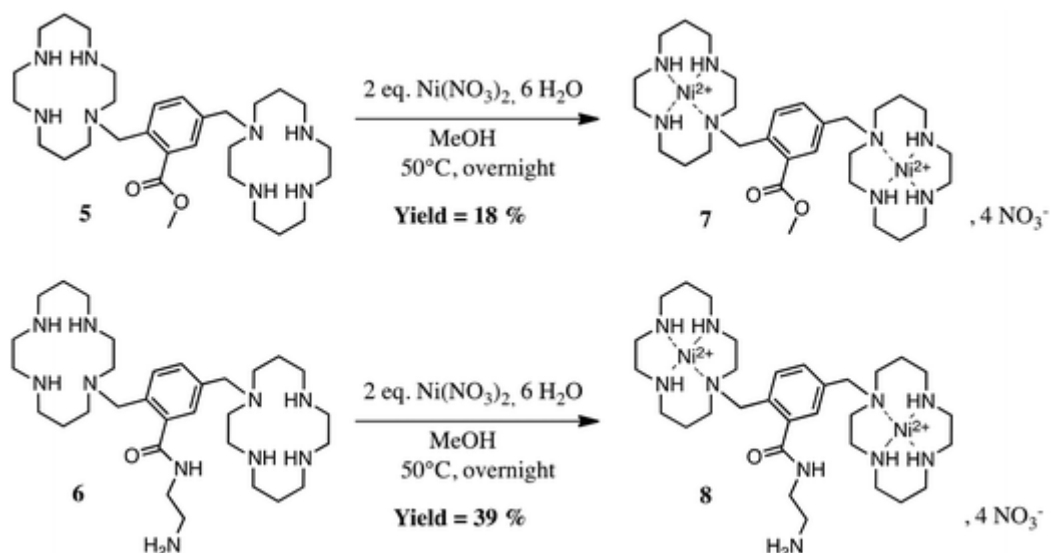
AMD3100 derivative **3** is obtained in 82% yield, after condensation of two equivalents of tris(Boc)cyclam on compound **2** in the presence of a base ([Scheme 3](#)). Nucleophilic attack of ethylenediamine on the ester function gives access to **4** after 6 days at 60 °C. Compounds **3** and **4** are then deprotected in acidic condition to form respectively **5** and **6** in good yields.



Scheme 3 Synthesis of new AMD3100 analogues functionalised with an ester and an ethylenediamine group.

As it has been shown that the incorporation of Ni²⁺ in the bicyclam AMD3100 enhances the binding to the chemokine receptor by 50-fold,²² we investigated the metal complex formation of our analogues. Additionally, Ni²⁺-cyclam complexes are known to be particularly inert due to their stability constants (log *K*) indicative of high thermodynamic stability (19.9–20.3)²³ and their slow kinetics of dissociation.²⁴ The complexes persist almost indefinitely even in strong acidic solutions and the only reported method to remove Ni²⁺ from cyclam involves cyanide at high temperature.

Thus, after deprotonation of **5** and **6** with NaOH (16 M) and extraction with chloroform, two equivalents of Ni(NO₃)₂·6H₂O were added to obtain the corresponding Ni²⁺ complexes ([Scheme 4](#)). Purification by reverse phase chromatography to remove any trace of free nickel(II) was performed to obtain **7** and **8** in 18% and 39% yield respectively. Yields are low in these cases due to the purification process. In order to investigate if ethylenediamine pendant arm coordinates one of the nickel atoms in compound **8**, UV-Visible absorption spectra was recorded in PBS at room temperature (see [ESI†](#)). The latter shows a band at 460 cm⁻¹, characteristic of a low-spin Ni^{II} tetramine complex. The amino pendant arm is therefore not involved in the coordination sphere of nickel.²⁵



Scheme 4 Nickel(II) complex formation of the AMD3100 analogues.

Biological assays: antibody competition, calcium signalling and anti-HIV activity

Cellular binding assays of our AMD3100 analogues to the CXCR4 receptor were investigated in a competition assay with an anti-CXCR4 monoclonal antibody (mAb) (12G5 conjugated to Phycoerythrin). A T-lymphocyte cell line (Jurkat) that expresses high levels of the CXCR4 receptor was used and the binding of compounds **5**, **6**, **7** and **8** to the cells are analysed by flow cytometry. The binding assay is carried out by saturation of the cells' receptors with a high concentration of analogues (*ca.* 20 μ M). After incubating with a saturating concentration of the antagonist, cells are washed to remove the excess of unbound compound and the specific fluorescent antibody is introduced. After a second incubation, cells are washed to remove the excess of antibody and compound displaced by the antibody. Then, cells are analysed by flow cytometry. The Mean Fluorescent Intensity (MFI) is used as a measure of binding and a quantitative way of calculating the inhibition percentage of mAb binding. AMD3100 is used as a reference compound. The non-metallated ligands **5** and **6** both show a significant decrease in the inhibition percentage compared to AMD3100 with 45% and 46% respectively ([Table 1](#)) ([Fig. 2](#)). Incorporation of a metal ion into the macrocyclic rings of AMD3100 analogues increases binding affinity to CXCR4, complexes **7** and **8** show higher inhibition percentages, 73% and 84% respectively, than the non-metallated ligands ([Table 1](#)) ([Fig. 2](#)). This is in agreement with Bridger and co-workers studies.²² A mutational analysis of the CXCR4 binding site for AMD3100 has identified

amino acid Asp¹⁷¹ and Asp²⁶² as key residues involved in the binding to the CXCR4 receptor.¹¹ The carboxylate groups of the receptor residues form three (one strong, one intermediate and one weak) hydrogen bonds with protonated cyclam of AMD3100. It was later determined that the increased binding affinity of the metal ion substituted AMD3100 is obtained through enhanced interaction of one of the cyclam ring systems with carboxylate group of Asp²⁶².²² With metal complexes, coordination of the carboxylate oxygens to the metal centre can occur while one weaker hydrogen bond to a nitrogen atom in the cyclam ring remains. Coordination interactions are stronger interactions than hydrogen bonding. Hence they are thought to be the dominant interactions for metal complexes. Complexes **7** and **8** should have stronger interactions with the CXCR4 receptor as aspartate residue coordinates nickel(II), resulting in higher inhibition percentages compared to their unmetalated ligands **5** and **6**. Even if the functionalisation of our AMD3100 analogues disrupted the affinity towards CXCR4, the incorporation of nickel(II) in the cyclam cavities has a positive effect resulting in inhibition percentages close to those observed for the reference compound AMD3100. If we compare the different functionalisations of the complexes **7** and **8**, the ethylenediamine analogue has a slightly higher inhibition percentage, which may be due to more flexible pendant arm that can form hydrogen bonds more easily.

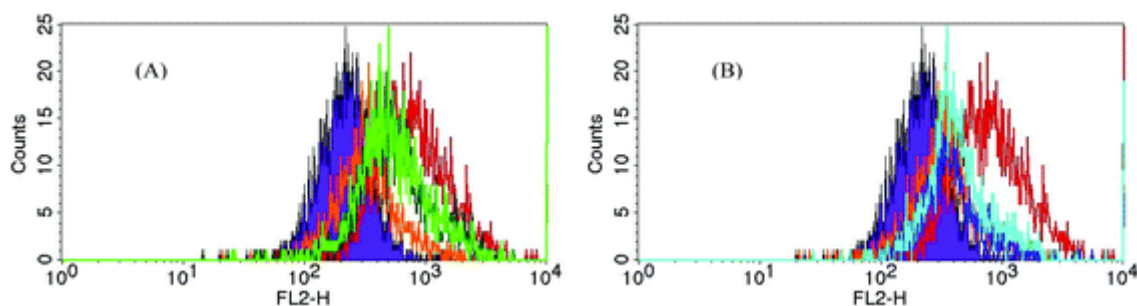


Fig. 2 Flow cytometric histogram plots for the binding of 12G5 mAb in competition with compound **5** (light green) and **6** (dark green) (A) and with compounds **7** (light blue) and **8** (dark blue) (B). Negative control (purple), positive control (red) and binding of 12G5 mAb in competition with AMD3100 (orange) are shown.

Table 1 Inhibition of anti-CXCR4 mAb (clone 12G5) binding to CXCR4⁺ jurkat cells

Compound	Control	MFI ^a	Inhibition percentage
----------	---------	------------------	-----------------------

Compound	Control	MFI ^a	Inhibition percentage
<i>a</i> Mean fluorescent intensity used to calculate the amount of antibody bound to CXCR4.			
	Negative	344.67	
5		708.57	45%
6		704.29	46%
7		524.78	73%
8		451.59	84%
AMD3100		413.90	90%
	Positive	1005.00	

Further biological characterisation was carried out to determine the impact of the antagonism of the receptor in signalling processes and the use of the receptor for viral cell entry. Prevention of signal transduction by the natural ligand is a useful indicator of cellular targeting and would inhibit activation of cell recruitment. Signal inhibition was validated by measurement of the intracellular calcium concentration increase, which is a downstream effect of CXCR4 receptor activation by its specific chemokine ligand CXCL12.²⁶ AMD3100 and the copper(II) complex of AMD3100 were included as controls, see [Table 1](#). The anti-HIV assay was used to co-validate the signalling data, as this is a well-established assay, which provides further information on the antagonist characteristics. The anti-HIV-1 (X4 HIV-1 NL4.3) activity of these compounds was determined in CD4⁺CXCR4⁺ human T cells using the well-documented HIV-1 infection assay (see [Table 2](#)).²⁷

Table 2 Anti-HIV X4 activity and inhibition of CXCL12-induced calcium signalling (in μM)

Compound	Anti-HIV-1 (EC_{50}) ^a	Ca ²⁺ flux CXCR4 (IC_{50}) ^b
AMD3100	0.011	0.120
Cu ₂ AMD3100	0.062	0.113
5	0.150	0.340
6	0.295	0.929
7	0.710	1.20

a EC_{50} is the effective concentration (in μM) to reduce the cytopathic effect of the CXCR4-using (X4) HIV-1 strain NL4.3 by 50% in MT-4 cells. *b* IC_{50} is the inhibitory concentration of the compound (in μM) required to inhibit 50% of the CXCL-12 (SDF-1) induced Ca²⁺ signalling in the CXCR4-transfected U87 cell line.

Compound	Anti-HIV-1 (EC ₅₀) ^a	Ca ²⁺ flux CXCR4 (IC ₅₀) ^b
8	0.095	0.016
10	0.845	—
11	4.50	—
12	0.800	—

As already mentioned, the chelator units would be expected to interact with aspartate residues on the CXCR4 chemokine receptor surface *via* H-bonding and electrostatic interactions and the metal complexes would form coordinate bonds.²² In the signalling assay we can compare compounds **5** and **7** showing in this case that the coordination of nickel(II) does not increase the affinity of our compounds for CXCR4 as was observed for the same compounds in the flow cytometry study. This result correlates with the anti-HIV infection assay although both still demonstrate sub- μ M values. Compounds **6** and **8** show increased potency of the nickel(II) complex in both calcium signalling and antiviral assays, which is consistent with antibody competition assay. With an IC₅₀ of 16 nM, **8** presents a higher potency, compared to both AMD3100 and its copper(II) complex which both have IC₅₀ values >100 nM. The presence of the appended amino group may be responsible for this bonding impact as it will be an effective hydrogen bond donor for interaction with the aspartate/glutamate rich surface of the CXCR4 receptor.

Overall, although the AMD3100 type structure has been modified by the introduction of functional groups on the phenyl moiety, compounds **6** and **8** can be considered as highly effective CXCR4 antagonists and we can now consider the introduction of a probe component for molecular imaging into these structures.

Towards molecular imaging: introduction of an imaging probe component

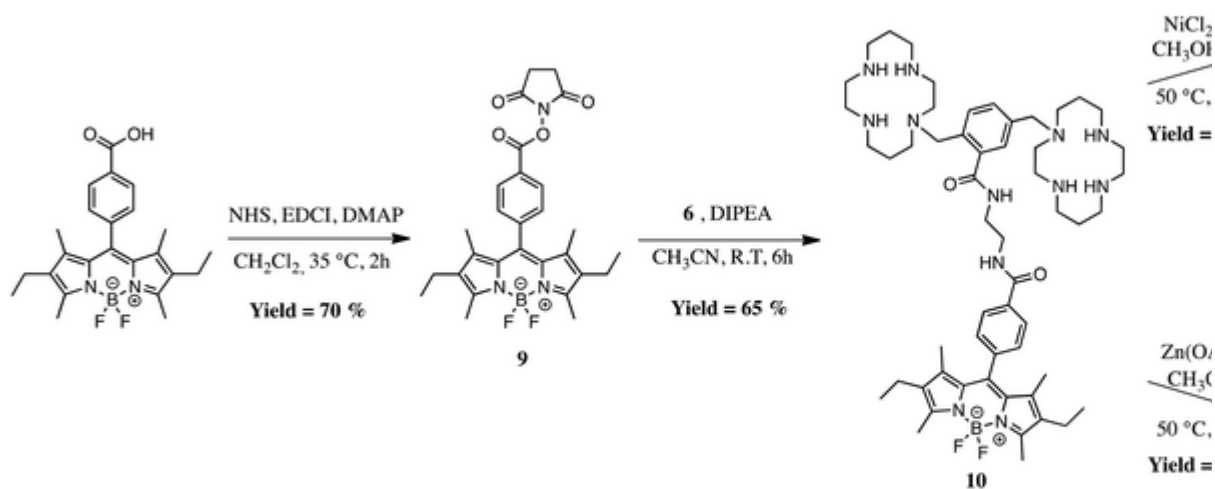
Efficient syntheses towards functionalised AMD3100 were developed whilst maintaining strong anti-HIV potency and CXCR4 affinity. Both amine analogues **6** and **8** can be used to conjugate the AMD3100 moiety to an imaging probe as the primary amine enables coupling reactions with carboxylic acid, active ester or anhydride. Two different imaging probe components were attached, a fluorescent moiety and a PET isotope radiolabelling precursor.

The main advantage for PET imaging here is to introduce the radiolabelling site by AMD3100 functionalisation rather than using the cyclam cavity to chelate a radiometal as it has already been described and shows low *in vivo* stability.¹⁷ Cyclam can form complexes that are thermodynamically stable *in vitro* but it has been shown that transchelation of the radiometal to ceruloplasmin and ultimately superoxide dismutase (SOD) can occur *in vivo* in the case of ⁶⁴Cu,²⁸ resulting in accumulation of the radioisotope in the blood and liver.^{17c}

Introduction of a BODIPY dye

Amongst the options for fluorescent imaging components, borodipyrrromethane type dyes (4,4-difluoro-4-borata-3a-azonia-4a-aza-s-indacene, abbreviation BODIPY®) exhibit high stability, high extinction coefficients, sharp emission bands and high quantum yields.²⁹ Additionally, BODIPYs emission can be shifted to the red-NIR region by extending the π -conjugation of the central core³⁰ and water soluble dyes can be obtained by addition of sulfonic acid moieties³¹ or coupling to an azamacrocycle.³² With all of these attractive properties, BODIPYs appear to be an excellent choice as an optical imaging component and a BODIPY carrying an activated ester was prepared to couple to the amine AMD3100 analogue **6**.

Starting from BODIPY-acid, the corresponding *N*-hydroxysuccinimidyl ester was obtained upon reaction with NHS in the presence of EDCI in dichloromethane at room temperature in 70% yield ([Scheme 5](#)).³³ The subsequent coupling of the activated ester with **6** yields **10** in a 65% yield after purification by column chromatography. Compound **10** was labelled with Ni²⁺ and Zn²⁺ by adding two equivalents of appropriate metal salts. It has to be noted that, in this case, the zinc complex was also synthesised, in order to study the influence of the metal on the fluorescence of the compound. Moreover, Zn²⁺ also strongly increases the affinity of AMD3100 for the CXCR4 receptor.²² Both complexes **11** and **12** were isolated in almost quantitative yield. One important point is that these BODIPY-AMD3100 analogues are water-soluble without the requirement for any solubilising agent (such as DMSO), which is crucial for biological applications such as molecular imaging. Indeed, one main drawback for the use of BODIPY dyes in medical imaging is their very poor solubility in water. It is still currently challenging to introduce, in a simple synthetic manner, solubilising groups for biological applications.



Scheme 5 Synthesis of Bodipy-AMD3100 analogues.

Anti-HIV assays were carried out with compounds **10**, **11** and **12**. These experiments showed that the introduction of the fluorescent probe induced a reduction of the anti-HIV activity, although **10** and **12** still maintained sub- μM activity levels, see [Table 2](#). It was interesting to note that the nickel(II) complex (**11**) was again less active than the metal-free chelator **10**. This suggests that the geometric preferences of the nickel(II) ion on binding to CXCR4 protein aspartate/glutamate side chains may be disrupted by functionalisation of the central phenyl ring. Zinc(II) is d^{10} and is more flexible in its coordination geometry. This may account for the higher activity of **12** compared to **11**, which is more similar to the metal-free chelating unit **10**.

The photophysical properties of the different BODIPY-AMD derivatives were studied in PBS at room temperature. The data are collected in [Table 3](#). All compounds exhibit two absorption bands characteristic of the BODIPY signature, which consists of the S_0-S_1 feature placed near 525 nm and the S_0-S_2 one located near 380 nm, both readily assigned to spin-allowed $\pi-\pi^*$ transitions. It is important to note that no aggregation can be observed in PBS, which is mainly characterised by a broadening of the absorption band as well as a dual

absorption. The ϵ (λ) values of the Ni(II) and Zn(II)-AMD3100-BODIPY **11** and **12**, are relatively high, ranging from 30 200 to 53 900 M⁻¹ cm⁻¹, those of free ligand **10** is a little lower (16 500 M⁻¹ cm⁻¹).

Table 3 Photophysical properties of the BODIPY derivatives in PBS at 298 K

Compound	λ_{abs} (nm)	λ_{em} (nm)	ϵ (M ⁻¹ cm ⁻¹)	Φ	Brightness ^b (M ⁻¹ cm ⁻¹)
<i>a</i> The quantum yields, Φ_F , were measured at 298 K, using rhodamine 6G ($\Phi_F = 0.78$ in water, $\lambda_{\text{exc}} = 488$ nm). <i>b</i>					
Brightness = $\Phi \times \epsilon$.					
10	525	539	16 452	5	822
11	524	540	53 872	7	3771
12	524	540	30 167	27	8145

As an example, [Fig. 3](#) exhibits the absorption, emission and excitation spectra of compound **12** (see ESI† for all spectra). The Φ_F value of the AMD3100-BODIPY **10** is relatively low, mainly because of the presence of several amine functions and a flexible linker between the BODIPY and the AMD3100 part (“loose bold effect”). Complexation of the Bodipy-AMD3100 analogue with Zn²⁺ (which naturally occurs when injecting AMD3100 *in vivo*), resulted in a consequent enhancement of the fluorescence, yielding to a quantum yield of 27% and a brightness of 8200 M⁻¹ cm⁻¹, which is sufficient for at least *in vitro* fluorescence imaging.³⁴ Concerning the nickel complex **11**, the fluorescence is still relatively low ($\Phi = 7\%$). Further investigations would be needed to explain this phenomena, which may be due to a paramagnetic character of Ni^{II}. Nevertheless, the brightness of the compound (almost 4000 M⁻¹ cm⁻¹) is sufficient for biological applications.

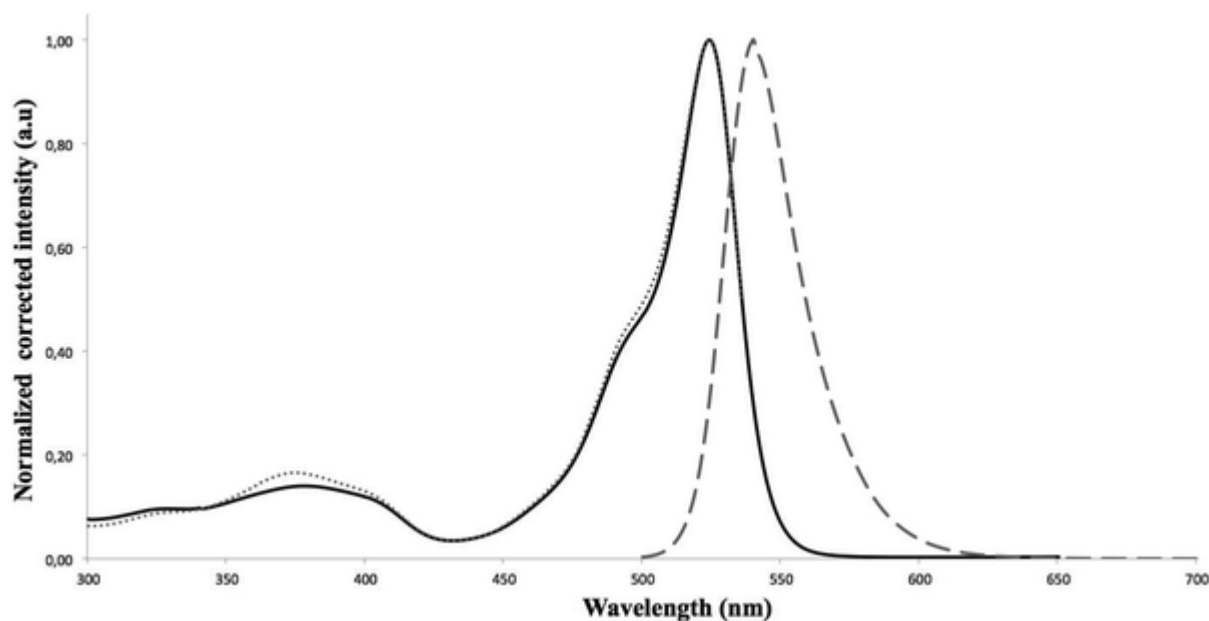
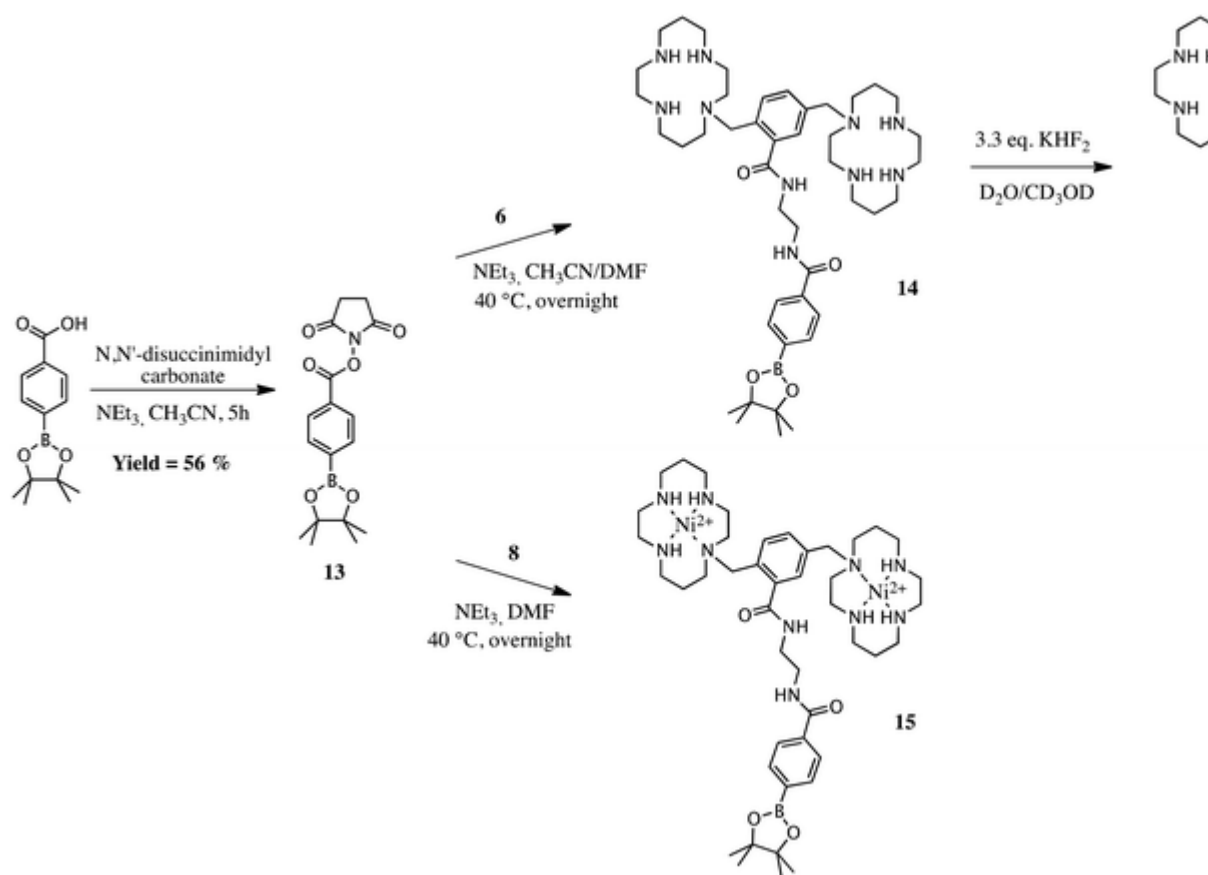


Fig. 3 Absorption (plain line), emission (large dashed line) and excitation (small dashed line) spectra of compound **11**.

Introduction of a precursor for radiofluorination

Fluorine-18 has gained prominence in PET imaging in the last decades due to its widespread availability, relatively low cost of production and its optimal nuclear and chemical properties, *i.e.* low positron energy (635 keV), high abundance, and relatively long half-life (109.7 min) when compared to ^{11}C .³⁵ Nevertheless with a half-life of 109.7 min, the synthesis of labelled imaging agents needs to be rapid and efficient. The B–F bond is one of the strongest bonds known, Ting *et al.* developed a pinacol phenylboronate diester able to react with F^- in a single, rapid and high-yielding step at pH 4–7 in aqueous solvents and at temperatures that are unlikely to denature biomolecules.³⁶ Inspired by this work, the pinacol phenylboronate diester PET precursor was coupled to the functionalised compounds **6** and **8** ([Scheme 6](#)).



Scheme 6 Synthesis of AMD3100 pinacol phenyl boronate analogues as PET precursors and AMD3100 trifluoroborate.

Starting from a commercially available product, 4-(4,4,5,5-tetramethyl-1,3,2-dioxaborolan-2-yl)benzoic acid, an activated ester **13** of the pinacol phenylboronate diester is synthesised by reaction with *N,N'*-disuccinimidyl carbonate and triethylamine in a 56% yield. Nucleophilic attack of **6** and **8** gives the resulting AMD3100 analogues **14** and **15** that constitute two precursors for ¹⁸F radiolabelling. It has to be noted that **15** was synthesised starting from compound **8** and not by metallation of **14**, because the pinacol boronate intermediate was subject to hydrolysis during the metallation step.

Fluoride treatment was performed on **14** to validate our concept. Following a previous reported protocol,³⁵ **14** was dissolved in a small volume of deuterated methanol and an aqueous solution of KHF₂ (3.3 eq.) was added. The solution turned immediately cloudy and further deuterated methanol was added to dilute the solution. The reaction mixture was stirred for 30 min at room temperature and the reaction was followed by ¹¹B and ¹⁹F NMR. The ¹¹B signal was shifted from 31.6 ppm to 0.4 ppm and appeared as a quadruplet due to the coupling between boron and fluorine. In the ¹⁹F NMR, the consumption of KHF₂ was

evidenced by the disappearance of the signal at -170 ppm and the presence of a signal at -142.7 ppm, characteristic of a $-\text{BF}_3$. Fluorination was also confirmed by mass spectrometry. This experiment confirms the high reactivity of the pinacol phenylboronate derivatives and their potential as precursors for the synthesis of ^{18}F radiopharmaceuticals.

Conclusion

A series of novel CXCR4 antagonists have been synthesised in this work and it has been demonstrated that functionalisation of the central bridging phenyl group in AMD3100 can be carried out without significant loss in the affinity for the CXCR4 receptor. The compounds have been characterised as sub- μM antagonists in a series of assays demonstrating effective binding to the receptor *in vitro*. They have then been modified for imaging applications *via* addition of a prosthetic group for radiofluorination or a fluorescent dye molecule to delineate the route to application. This design separates out the targeting and imaging components of the molecule, which is in contrast to the previously described complexes of AMD3100 with radiometals. The modular approach is advantageous in tuning for different modalities and optimum receptor ‘on’ and ‘off’ binding rates. There is also the potential for multimodal imaging to allow evaluation of the compounds by a range of imaging techniques to more precisely characterise the interactions from a cellular level up to *in vivo* studies. The next steps for this study are to select the optimal candidates, optimise the radiolabelling conditions and carry out preliminary *in vivo* studies. In addition, the affinity towards CXCR7 of the novel compounds is under evaluation to determine the binding profile with this important and related chemokine receptor target.

Experimental section

Synthetic procedures

General information. Additional experimental details, data for compounds **1–16** (NMR, MS spectra and HPLC chromatograms) are given in ESI.[†]

Material. TriBocCyclam was generously donated by CheMatech and all other chemicals were purchased from Acros and Aldrich and were used without further purification. Organic solvents were removed under reduced pressure using rotary evaporator. Water was removed by lyophilisation.

Methyl-2,5-dimethylbenzoate (1). A mixture of 2,5-dimethylbenzoic acid (10.0 g, 66.6 mmol), sulphuric acid (14 mL, 13.3 mmol), and methanol (27 mL) was heated at reflux for 4 h. The mixture was poured into water (250 mL) and extracted with ethyl acetate (2 × 200 mL). The pooled organics were washed with saturated sodium bicarbonate (2 × 50 mL) and brine (50 mL), dried over MgSO₄, and concentrated *in vacuo* to give **1** (10.1 g, 92%) as a colorless oil. ¹H NMR (300 MHz, CDCl₃, 300 K): δ = 7.70 (d, ⁴J (H,H) = 1.7 Hz, 1H; CH), 7.18 (dd, ³J (H,H) = 7.9 Hz, ⁴J (H,H) = 1.4 Hz, 1H; CH), 7.10 (d, ³J (H,H) = 7.9 Hz, 1H; CH), 3.86 (s, 3H; OCH₃), 2.53 (s, 3H; CH₃), 2.32 ppm (s, 3H; CH₃); ¹³C{¹H} NMR (75 MHz, CDCl₃, 300 K): δ = 168.4 (C=O), 137.2 (Car), 135.4 (Car), 132.9 (CHar), 131.8 (CHar), 131.2 (CHar), 129.6 (Car), 51.9 (OCH₃), 21.4 (CH₃), 20.9 ppm (CH₃); ESI-MS: *m/z*: 165.31 [M + H]⁺.

Methyl-2,5-bis(bromomethyl)benzoate (2). To a solution of **1** (10.1 g, 61.6 mmol) in carbon tetrachloride (300 mL) were added *N*-bromosuccinimide (23.0 g, 129.3 mmol) and benzoyl peroxide (1.0 g, 4.1 mmol). The reaction mixture was heated at reflux for 4 h. The resulting suspension was filtered, and the residue was washed with chloroform (3 × 150 mL). The pooled organics were concentrated *in vacuo* to give a mixture of product and succinimide as determined by ¹H NMR. The mixture was dissolved in dichloromethane (600 mL) and washed with water (3 × 150 mL). The dichloromethane phase was dried over MgSO₄ and concentrated *in vacuo*, and the resulting residue was purified by reverse phase flash chromatography on C₁₈. After evaporation of acetonitrile, the aqueous solution was freeze dried to give **2** (13.9 g, 70%) as a white solid. ¹H NMR (500 MHz, CDCl₃, 300 K): δ = 8.00 (d, ⁴J (H,H) = 1.8 Hz, 1H; CH), 7.53 (dd, ³J (H,H) = 7.8 Hz, ⁴J (H,H) = 1.8 Hz, 1H; CH), 7.46 (d, ³J (H,H) = 7.8 Hz, 1H; CH), 4.94 (s, 2H; CH₂), 4.49 (s, 2H; CH₂), 3.98 ppm (s, 3H; OCH₃); ¹³C{¹H} NMR (75 MHz, CDCl₃, 300 K): δ = 166.6 (C=O), 139.6 (Car), 138.5, 133.2 (CHar), 132.5, 132.0, 129.7 (Car), 52.6 (OCH₃), 32.0 (CH₂), 31.0 ppm; ESI-MS: *m/z*: 322.54 [M + H]⁺.

AMD3100 Boc-ester (3). To a solution of tris-*tert*-butyl-1,4,8,11-tetraazacyclotetradecane-1,4,8-tricarboxylate (2.00 g, 3.98 mmol) in acetonitrile (20 mL) was added K₂CO₃ (1.38 g, 9.99 mmol) and compound **2** (0.63 g, 1.99 mmol). The reaction mixture was heated at 40 °C overnight. After cooling, the solution was filtered on celite. The solvent was evaporated and the resulting oil was taken up in 200 mL of diethylether, washed with 2 × 50 mL of water, dried over MgSO₄ and concentrated *in vacuo*. The resulting residue was purified by flash chromatography (A: CH₂Cl₂, B: CH₃OH, B 35%) to give **3** (1.89 g, 82%) as a white foam. m.p. 89 ± 1 °C; ¹H NMR (300 MHz, CDCl₃, 300 K): δ = 7.66 (s, 1H; CH), 7.43 (d, ³J (H,H) =

7.7 Hz, 1H; CH), 7.31 (d, 3J (H,H) = 7.7 Hz, 1H, CH), 3.85 (s, 3H; OCH₃), 3.81 (s, 2H; CH₂Ph), 3.51 (s, 2H; CH₂Ph), 3.45–3.14 (m, 23H), 2.67–2.52 (m, 4H), 2.45–2.28 (m, 4H), 1.94–1.77 (m, 4H; CH₂β), 1.70–1.61 (m, 4H; CH₂β), 1.50–1.24 ppm (m, 54H; CH₃); ¹³C{¹H} NMR (125 MHz, DMSO, 343 K): δ = 167.4 (C=O), 154.5 (*2), 154.4, 154.3 (*2), 154.2, 138.1 (Car), 137.5 (Car), 131.3 (Car), 130.3 (CHar), 129.7 (CHar), 129.6 (CHar), 78.4, 78.3, 78.2, 78.1, 78.0 (*2), 57.8, 56.2, 52.7, 52.5, 51.3, 51.1, 46.7, 46.6, 46.5(*3), 46.2, 46.0, 45.9 (*2), 45.8, 45.7, 45.5, 45.4, 27.8 (*12) (CH₃), 27.7 (*3) (CH₃), 27.6 (*3) (CH₃), 25.9 (*2) (CH₂β), 25.6 pm (*2) (CH₂β); ESI-MS: *m/z*: 1183.76 [M + Na]⁺, 1199.73 [M + K]⁺; HRMS (ESI): *m/z* calcd for C₆₀H₁₀₄N₈O₁₄ + Na⁺: 1183.7571, found 1183.7564; elemental analysis calcd (%) for C₆₀H₁₀₄N₈O₁₄: C 62.04, H 9.02, N 9.65; found: C 61.62, H 8.98, N 9.55; HPLC: *t_r* = 8.13 min, purity 98%.

AMD3100 Boc-ethylenediamine (4). Compound **3** (1.89 g, 1.63 mmol) was dissolved in distilled ethylenediamine (6.5 mL). The mixture was stirred at 40 °C for 7 days. The mixture was concentrated by evaporation and the resulting oil was taken up in acetone (200 mL). After filtration, the pooled organics were concentrated *in vacuo* to give a yellow foam. The resulting residue was purified by flash chromatography on silica gel (A: CH₂Cl₂, B: CH₃OH, B 15%) to furnish **4** (0.77 g, 40%) as a white foam. m.p. 98 ± 1 °C; ¹H NMR (500 MHz, CDCl₃, 324 K): δ = 8.17 (br.s, 1H; NHC=O), 7.49 (s, 1H; CH), 7.25 (d, 3J (H,H) = 7.3 Hz, 1H; CH), 7.20 (d, 3J (H,H) = 7.6 Hz, 1H; CH), 3.64 (s, 2H, CH₂Ph), 3.50 (s, 2H, CH₂Ph), 3.46 (q, 3J (H,H) = 6.0 Hz, 2H; CH₂NHC=O), 3.40–3.16 (m, 24H), 2.93 (t, 3J (H,H) = 6.0 Hz, 2H; CH₂NH₂), 2.66 (t, 3J (H,H) = 6.5 Hz, 2H), 2.60–2.52 (m, 2H), 2.46 (t, 3J (H,H) = 6.5 Hz, 2H), 2.40 (t, 3J (H,H) = 5.7 Hz, 2H), 2.10 (s, 2H), 1.89–1.77 (m, 4H; CH₂β), 1.71–1.61 (m, 4H; CH₂β), 1.44–1.39 (m, 36H; CH₃), 1.37–1.24 ppm (m, 18H; CH₃); ¹³C{¹H} NMR (125 MHz, CDCl₃, 324 K): δ = 169.9 (C=O), 156.1, 156.0, 155.9 (*2), 155.7 (*2), 138.7 (C_{ar}), 137.4 (C_{ar}), 135.1 (C_{ar}), 131.2 (CH_{ar}), 130.5 (CH_{ar}), 129.3 (CH_{ar}), 80.0, 79.9 (*2), 79.8 (*2), 79.7, 59.6 (CH₂), 58.0, 53.5, 52.5, 52.4, 52.1, 51.1, 50.9, 48.1 (*2), 48.0, 47.5, 47.3 (*2), 46.9, 46.5, 43.1 (*2), 42.1 (*2), 28.9 (*3) (CH₃), 28.8 (*9) (CH₃), 28.7 (*3) (CH₃), 28.6 (*3) (CH₃), 27.2 (*2) (CH₂β), 26.1 ppm (*2) (CH₂β); ESI-MS: *m/z*: 1189.82 [M + H]⁺; HRMS (ESI): *m/z* calcd for C₆₁H₁₀₈N₁₀O₁₃ + H⁺: 1189.8170, found 1189.8212; elemental analysis calcd (%) for C₆₁H₁₀₈N₁₀O₁₃: C 61.59, H 9.15, N 11.77; found C 61.17, H 9.43, N 11.51; HPLC: *t_r* = 8.48 min, purity 96%.

AMD3100-ester (5). A solution of 3 M HCl (3.0 mL) was added to **3** (100.0 mg, 0.08 mmol) and the reaction mixture was stirred for one hour. The resulting product was left one night at room temperature. The acid was evaporated *in vacuo* giving **5** + 6HCl + 10H₂O. (60.7 mg,

yield = 73%) as a white foam. ^1H NMR (300 MHz, D_2O , 300 K): δ = 8.32 (d, $^4J(\text{H,H}) = 1.8$ Hz, 1H), 7.88 (dd, $^3J(\text{H,H}) = 7.8$ Hz, $^4J(\text{H,H}) = 1.8$ Hz, 1H), 7.76 (d, $^3J(\text{H,H}) = 7.8$ Hz, 1H), 4.46 (br.s, 2H), 3.98 (s, 3H; OMe), 3.92–3.81 (m, 2H), 3.76–3.53 (m, 17H), 3.49–3.28 (m, 15H), 2.29–2.12 ppm (m, 8H); $^{13}\text{C}\{^1\text{H}\}$ NMR (75 MHz, D_2O , 300 K): δ = 168.1, 135.9, 134.9, 134.2, 133.4, 131.2, 131.0, 48.2, 47.9, 45.5, 44.8, 42.1, 41.6, 41.5, 40.8, 40.7, 38.44, 38.38, 38.0, 37.2, 36.8, 19.1 ($\text{CH}_2\beta$), 19.0, 18.5, 17.9 ppm; HRMS (ESI): m/z calcd for $\text{C}_{30}\text{H}_{56}\text{N}_8\text{O}_2 + \text{H}^+$: 561.4599, found 561.4573; elemental analysis calcd (%) for $\text{C}_{30}\text{H}_{56}\text{N}_8\text{O}_2 + 10\text{H}_2\text{O} + 6\text{HCl}$: C 37.54, H 8.61, N 11.68; found C 37.82, H 8.05, N 11.65; HPLC: $t_r = 5.53$ min, purity 97%.

AMD3100-ethylenediamine (6). Compound **4** (0.47 g, 0.40 mmol) was dissolved in a solution of 3 M HCl (10 mL). The mixture was stirred overnight at room temperature. The mixture was evaporated, taken up in acetone (50 mL) and then stirred overnight. The precipitate was filtered, washed with acetone and ether and finally dried *in vacuo*. The compound **6** + 9HCl + 5H₂O was obtained as a white solid (400 mg, yield = 100%). ^1H NMR (300 MHz, D_2O , 300 K): δ = 7.93–7.91 (s, 1H), 7.81–7.74 (m, 2H), 4.51 (s, 2H; CH_2Ph), 4.29 (s, 2H; CH_2Ph), 3.82–3.78 (m, 2H), 3.67–3.34 (m, 32H), 3.18–3.14 (m, 2H), 2.27–2.16 ppm (m, 8H; $\text{CH}_2\beta$); $^{13}\text{C}\{^1\text{H}\}$ NMR (75 MHz, D_2O , 300 K): δ = 171.0 (C=O), 135.7 (CHar), 134.5 (CHar), 134.4 (CHar), 133.4 (Car), 131.6 (Car), 130.2 (Car), 58.1, 57.5, 48.4, 47.9, 47.8, 45.6, 45.3, 45.0, 42.1, 41.8, 41.7, 41.2, 41.0, 38.9, 38.7, 38.5, 38.1, 37.8, 37.7, 37.6, 19.3 ($\text{CH}_2\beta$), 19.2 ($\text{CH}_2\beta$), 18.8 ($\text{CH}_2\beta$), 18.5 ppm ($\text{CH}_2\beta$); HRMS (ESI): m/z calcd for $\text{C}_{31}\text{H}_{60}\text{N}_{10}\text{O} + \text{H}^+$: 589.5024, found 589.5034; elemental analysis calcd (%) for $\text{C}_{31}\text{H}_{61}\text{N}_{10}\text{O} + 9\text{HCl} + 5\text{H}_2\text{O}$: C 36.97, H 7.91, N 13.91; found C 37.13, H 8.06, N 14.33.

Few drops of NaOH (16 mol L⁻¹) were added on compound **6** + 9HCl + 5H₂O in order to obtain a viscous solution and chloroform (100 mL) was added quickly. The two layers were separated and the organic layer was dried over magnesium sulfate. After evaporation of the solvent, **6** + 9.5H₂O (276 mg, yield = 91%) was obtained as a light yellow oil. ^1H NMR (300 MHz, CDCl_3 , 300 K): δ = 8.64 (t, $^3J(\text{H,H}) = 5.4$ Hz, 1H; NHC=O), 7.41 (d, $^3J(\text{H,H}) = 7.8$ Hz, 1H), 7.37 (d, $^4J(\text{H,H}) = 1.7$ Hz, 1H), 7.12 (dd, $^3J(\text{H,H}) = 7.8$ Hz, $^4J(\text{H,H}) = 1.7$ Hz, 1H), 3.51 (s, 2H; CH_2Ph), 3.37 (s, 2H; CH_2Ph), 3.32 (q, $^3J(\text{H,H}) = 5.9$ Hz, 2H; $\text{CH}_2\text{NHC=O}$), 2.76 (t, $^3J(\text{H,H}) = 6.2$ Hz, 2H; CH_2NH_2), 2.71–2.19 (m, 40H), 1.72 (quint, $^3J(\text{H,H}) = 5.5$ Hz, 2H; $\text{CH}_2\beta$), 1.63 (quint, $^3J(\text{H,H}) = 5.5$ Hz, 2H; $\text{CH}_2\beta$), 1.55–1.45 ppm (m, 4H; $\text{CH}_2\beta$); $^{13}\text{C}\{^1\text{H}\}$ NMR (75 MHz, D_2O , 300 K): δ = 170.5 (C=O), 137.9 (Car), 137.6 (Car), 135.7 (Car), 130.6 (CHar), 130.4 (CHar), 128.0 (CHar), 57.9 (CH_2Ph), 55.8 (CH_2Ph), 54.6, 54.2, 53.3, 53.2, 50.9, 50.5, 49.3, 49.1, 48.7, 48.6, 48.5, 48.3, 48.2, 47.8, 47.7, 47.3, 43.1, 41.9, 28.6 ($\text{CH}_2\beta$),

28.4 (CH₂β), 26.5 (CH₂β), 26.1 ppm (CH₂β); elemental analysis calcd (%) for C₃₁H₆₁N₁₀O + 9.5H₂O: C 48.99, H 10.48, N 18.43; found C 49.00, H 10.57, N 18.33; HPLC: *t*_r = 5.36 min, purity 99%.

Ni₂AMD3100-ester (7). 0.60 mL (0.06 mmol) of a titrated solution of Ni(NO₃)₂ · 6H₂O (*c* = 0.106 mol L⁻¹) in water were added to a solution of **5** (17.3 mg, 0.03 mmol) in a 3 mL mixture of MeOH–H₂O (9 : 1). The reaction was stirred at 50 °C overnight. After completion, reverse phase C₈ semi-preparative HPLC (A: H₂O) was performed to furnish **7** (3.7 mg, 18%) as a light orange foam. HRMS (ESI): *m/z* calcd for C₃₀H₅₄N₈Ni₂O₂ – 2H²⁺: 337.1533, found 337.1529; HPLC: *t*_r = 5.88 min, purity 95%.

Ni₂AMD3100-ethylenediamine (8). 15.0 mL (1.59 mmol) of a titrated solution of Ni(NO₃)₂ · 6H₂O (*c* = 0.106 mol.L⁻¹) in water were added to a solution of **6** + 9.5H₂O (568 mg, 0.79 mmol) in a 110 mL mixture of MeOH–H₂O (9 : 1). The reaction was stirred at 50 °C overnight. After completion, reverse phase C₁₈ flash chromatography (A: H₂O) was performed to furnish **8** + 4NO₃ + 7H₂O (332 mg, 39%) as a light orange foam. UV-Vis (PBS), λ (nm): 460; HRMS (ESI): *m/z* calcd for C₃₁H₅₈N₁₀Ni₂O – 2H²⁺: 351.1746, found 351.1740; elemental analysis calcd (%) for C₃₁H₅₈N₁₀Ni₂O + 4NO₃ + 9.5H₂O: C 34.59, H 6.56, N 18.22; found C 34.24, H 6.30, N 18.88; HPLC: *t*_r = 5.77 min, purity 88%.

Bodipy-NHS-ester (9)³⁰. 54 mg of *N*-hydroxysuccinimide (0.48 mmol), 58 mg of dimethylaminopyridine (DMAP) (0.48 mmol) and 92 mg of 1-(3-dimethylaminopropyl)-3-ethylcarbodiimide hydrochloride (EDCI) (0.48 mmol) were added to a solution of 4,4-difluoro-8-(4-carboxyphenyl)-1,3,5,7-tetramethyl-2,6-diethyl-4-bora-3a,4a-diaza-s-indacene (100 mg, 0.24 mmol) in CH₂Cl₂ (50 mL). The reaction was stirred at 35 °C. After complete activation of the acid function (2 h) followed by TLC, the mixture was washed with 2 × 10 mL of water, the organic phase was dried over MgSO₄ and the solvent was evaporated to give a red oil. The crude product was purified by chromatography on silica gel (AcOEt–Hexane 50 : 50). Upon concentration of the pure fraction, recrystallisation in a mixture of dichloromethane and hexane gave **9** as a red solid (88 mg, yield = 70%). ¹H NMR (300 MHz, CDCl₃, 300 K): δ = 8.23 (d, ³*J* (H,H) = 8.3 Hz, 2H; CHar_{Bod}), 7.47 (d, ³*J* (H,H) = 8.3 Hz, 2H; CHar_{Bod}), 2.92 (bs, 4H; CH₂C=O), 2.51 (s, 6H; CH₃), 2.27 (q, ³*J* (H,H) = 7.5 Hz, 4H; CH₂CH₃), 1.25 (s, 6H; CH₃), 0.96 ppm (t, 6H, ³*J* (H,H) = 7.5 Hz; CH₂CH₃); ¹³C{¹H} NMR (75 MHz, CDCl₃, 300 K): δ = 169.2 (*2) (NC=O), 161.4 (CO₂), 154.6 (*2) (C_{pyrrole}), 143.0 (Car_{Bod}), 138.7 (C_{Bod}), 138.0 (*2) (C_{pyrrole}), 137.7 (*2) (C_{pyrrole}), 133.3 (*2) (CHar_{Bod}), 131.2 (*2) (C_{pyrrole}), 129.3 (*2) (CHar_{Bod}), 125.6 (Car_{Bod}), 25.7 (*2) (CH₂C=O), 17.3 (*2) (CH₂CH₃), 14.6 (*2) (CH₂CH₃), 12.7 (*2) (CH₃), 12.1 ppm (*2); ¹¹B{¹H} NMR (192.5 MHz, CDCl₃, 300 K): δ

= 0.79 ppm (t, 1J (B,F) = 33.1 Hz); ESI-MS: m/z = 544.21 [M + Na]⁺; UV-Vis (CH₃CN), λ (nm) (ϵ , M⁻¹ cm⁻¹): 525 (73 000), 492 (sh, 23 200), 378 (7940); elemental analysis calcd (%) for C₂₈H₃₀BF₂N₃O₄: C 68.50, H 6.67, N 6.39; found C 68.78, H 6.87, N 5.95.

AMD3100-bodipy (10). Diisopropylethylamine (172 μ L, 1.04 mmol) was added to a solution of **6** (408 mg, 0.69 mmol) in acetonitrile (40 mL). A solution of bodipy **9** (694 mg, 0.69 mmol) in acetonitrile (10 mL) was then added and the mixture was stirred at room temperature during 6 h, until total consumption of the starting materials was observed by TLC. Solvent was evaporated, and the resulting red oil was purified by column chromatography on silica gel (eluent: CH₂Cl₂–EtOH–NH₄OH 20 : 60 : 20). Precipitation from CH₂Cl₂–hexane gave the desired compound **10** as a red solid (446 mg, yield = 65%) Mp: >200 °C; ¹H NMR (300 MHz, CDCl₃, 300 K): δ = 9.80–9.67 (bs, 1H), 8.62–8.49 (bs, 1H), 8.12 (d, 3J (H,H) = 8.2 Hz, 2H), 7.55 (d, 3J (H,H) = 7.7 Hz, 1H), 7.43 (s, 1H), 7.33 (d, 3J (H,H) = 8.2 Hz, 2H), 7.20 (d, 3J (H,H) = 7.7 Hz, 1H), 3.73–3.46 (m, 12H), 2.79–2.31 (m, 37H), 2.26 (q, 4H, 3J (H,H) = 7.5 Hz; CH₂CH₃), 1.92–1.52 (m, 8H), 1.32–1.24 (m, 9H), 0.94 ppm (t, 3J (H,H) = 7.5 Hz, 6H; CH₂CH₃); ¹³C{¹H} NMR (75 MHz, CDCl₃, 300 K): δ = 173.0 (NHC=O), 166.6, 154.3 (*2) (C_{pyrrole}), 139.8 (Car), 139.3 (Car_{Bod}), 139.2 (C_{Bod}), 138.3 (*2) (C_{pyrrole}), 138.2 (Car), 136.1, 134.5 (Car_{Bod}), 133.2 (*2) (C_{pyrrole}), 131.5 (CHar), 130.6 (*2) (C_{pyrrole}), 130.5 (CHar), 128.8 (*2) (CHar_{Bod}), 128.3 (*2), 127.2 (CHar), 58.3 (CH₂), 55.2, 54.9, 54.6, 54.2, 53.8, 53.2, 51.3, 51.1, 49.9, 49.4 (*2), 48.8, 48.6, 48.5, 48.4, 48.1, 47.1, 42.8, 39.7, 28.7 (CH₂ β), 28.6, 26.6, 26.2, 17.2 (*2) (CH₂CH₃), 14.8 (*2) (CH₂CH₃), 12.7 (*2) (CH₃), 12.0 ppm (*2); ¹¹B{¹H} NMR (96 MHz, CDCl₃, 300 K): δ = 0.76 ppm (t, 1J (B,F) = 33.6 Hz); ESI-MS: m/z = 995.7 [M + H]⁺, 1021.7 [M + Na]⁺, 1033.7 [M + K]⁺; HRMS (ESI): m/z calcd for C₅₅H₈₅BF₂N₁₂O₂ + H⁺: 995.7062, found 995.7012.

Ni₂AMD3100-bodipy (11). 3.1 mg of NiCl₂ (0.023 mmol) was added to a solution of 10.4 mg of compound **10** (0.012 mmol) in 6 mL of methanol. The mixture was stirred at 50 °C for 2 h. After evaporation, compound **11** was obtained as a red solid (14.2 mg, yield = 95%). ESI-MS: m/z = 555.27 [M – 2H – 4Cl]²⁺; HRMS (ESI): m/z calcd for C₅₅H₈₅BCl₄F₂N₁₂Ni₂O₂ – 2H – 4Cl²⁺: 555.2740, found 555.2699.

Zn₂AMD3100-bodipy (12). 4.7 mg of Zn(OAc)₂ · 2H₂O (0.021 mmol) was added to a solution of 9.5 mg of compound **10** (0.011 mmol) in 6 mL of methanol. The mixture was stirred at 50 °C for 2 h. After evaporation, compound **12** was obtained as a red solid (27.7 mg, yield = 97%). ESI-MS: m/z = 592.28 [M – H – 3(OAc)]²⁺; HRMS (ESI): m/z calcd for C₆₃H₉₇BF₂N₁₂O₁₀Zn₂ – H – 3(OAc)²⁺: 592.2783, found 592.2780.

Pinacol phenylboronate activate ester (13). Triethylamine (340 μL , 2.43 mmol) and *N,N'*-disuccinimidyl carbonate (310 mg, 1.21 mmol) were added to a solution of 4-(4,4,5,5-tetramethyl-1,3,2-dioxaborolan-2-yl)benzoic acid (200 mg, 0.81 mmol) in acetonitrile (20 mL). The reaction mixture was stirred at room temperature for 5 h. The solvent was evaporated *in vacuo* with a bath temperature lower than 35 °C. The resulting product was dissolved in dichloromethane and washed with a saturated solution of sodium bicarbonate. After drying over magnesium sulfate, the organic layer was evaporated *in vacuo* with a low temperature bath >35 °C. Chromatography on silica gel (A: Pentane, B: EtOAc, B 50%) gave **13** (0.157 g, 56%) as a white powder. ^1H NMR (300 MHz, CDCl_3 , 300 K): δ = 8.09 (d, 3J (H,H) = 8.1 Hz, 2H; $\text{CHar}_{\text{Bpinacol}}$), 7.90 (d, 3J (H,H) = 8.1 Hz, 2H; CHar_{NHS}), 2.86 (s, 4H; CH_2 NHS), 1.33 ppm (s, 12H; CH_3); $^{13}\text{C}\{^1\text{H}\}$ NMR (75 MHz, CDCl_3 , 300 K): δ = 169.4 (*2) (CC=O NHS), 162.1 (CC=O), 135.1 ($\text{C}_{\text{pinacol}}$), 129.6 (*4) (CH), 127.3 (C_{NHS}), 84.6 (*2) (CMe_2), 25.9 (*2) (CH_2), 25.0 ppm (*4) (CH_3); HRMS (ESI): m/z calcd for $\text{C}_{17}\text{H}_{20}\text{BNO}_6 + \text{Na}^+$: 368.1279, found 368.1274.

AMD3100-pinacol phenylboronate (14). **6** (26 mg, 0.04 mmol) was dissolved in a mixture of acetonitrile (600 μL) and DMF (20 μL), triethylamine (77 μL) was then added. The solution was stirred at room temperature for 10 min and **13** (15 mg, 0.04 mmol) was added to the reaction. After one night stirring at 40 °C, the solvent was evaporated under a nitrogen flux to give **14** which still contains traces of DMF and was directly used without any further purification step. ^1H NMR (500 MHz, CDCl_3 , 500 K): δ = 9.79–9.63 (bs, 1H; NH), 8.77–8.65 (bs, 1H; NH), 8.07 (dd, 3J (H,H) = 5.2 Hz, 4J (H,H) = 1.5 Hz, 2H), 7.75 (d, 3J (H,H) = 8.1 Hz, 1H), 7.72–7.65 (m, 1H), 7.63 (d, 3J (H,H) = 8.1 Hz, 1H), 6.63 (dd, 3J (H,H) = 5.1 Hz, 4J (H,H) = 1.5 Hz, 2H), 3.70–3.31 (m, 7H), 2.90–2.85 (m, 7H), 2.73–2.20 (m, 35H), 1.79–1.52 (m, 6H), 1.19 ppm (s, 12H); ^{11}B (160 MHz, CDCl_3 , 300 K): δ = 31.6 ppm; ESI-MS: m/z = 819.6 [M + H] $^+$; MALDI-TOF: m/z = 819.63 [M + H] $^+$.

Ni₂AMD3100-pinacol phenylboronate (15). **8** (20 mg, 0.02 mmol) was dissolved in DMF (3 mL) and triethylamine (25 μL) was added. The solution was stirred at room temperature for 10 min and **13** (8 mg, 0.02 mmol) was added to the reaction. After one night stirring at 40 °C, the solvent was evaporated *in vacuo* with a bath temperature lower than 35 °C to give **15**. MALDI-TOF: m/z = 931.36 [M – 3H] $^+$.

AMD3100-phenyltrifluoroboronate (16). **14** (0.04 mmol) was dissolved in methanol-d₄ (150 μL) and a solution of KHF_2 in D_2O (35 μL , c = 4 M) was added. The solution immediately turned blurry and 1 mL of methanol-d₄ was added. The mixture was stirred for 30 min and NMR was recorded on the crude product. ^1H NMR (500 MHz, CD_3OD , 500 K): δ

= 8.08 (d, 3J (H,H) = 7.5 Hz, 2H), 7.72–7.69 (m, 1H), 7.61–7.57 (m, 1H), 7.44 (bs, 1H), 6.87 (d, 3J (H,H) = 6.9 Hz, 2H), 3.80–3.61 (m, 6H), 3.23–3.15 (m, 7H), 3.14–3.03 (m, 7H), 2.99–2.87 (m, 10H), 2.76–2.54 (m, 12H), 2.02–1.76 ppm (m, 6H); ^{11}B (160 MHz, CD_3OD , 300 K): δ = 0.34 ppm (q, 1J (B,F) = 11.9 Hz); ^{19}F (202 MHz, CD_3OD , 300 K): δ = –142.7 ppm; ESI-MS: m/z = 759.5 [M – H][–].

Chemokine-induced calcium signalling assay

Ca^{2+} mobilisation assays were performed by the use of a fluorometric imaging plate reader (FLIPR) (Molecular Devices, Sunnyvale, USA) as described previously.²⁶ Briefly, U87.CXCR4- and U87.CCR5-transfected cells were loaded with the fluorescent calcium indicator Fluo-3 acetoxymethyl (Molecular Probes, Leiden, The Netherlands) in the appropriate culture medium for 45 min at 37 °C, after which the cells were washed three times in Hanks balanced salt solution buffer containing 20 mM HEPES and 0.2% bovine serum albumin (pH 7.4). The cells were then incubated in the dark at 37 °C for 15 min with the compounds. Changes in intracellular calcium concentration upon addition of CXCL-12 (SDF-1), the specific ligand for CXCR4, were simultaneously measured in all 96 wells in a black-wall microtiter plate and in real time with the FLIPR. The data were expressed as fluorescence units *versus* time and were analysed using the FLIPR Control Software (Molecular Devices) and IC_{50} values were calculated using GraphPad Prism 4.0 software (San Diego, CA).

Anti-viral assays

Anti-HIV activity and cytotoxicity measurements in MT-4 cells were based on the viability of cells that had been infected or not infected with the CXCR4-using (X4) HIV-1 strain NL4.3 and exposed to various concentrations of the test compound. After the MT-4 cells were allowed to proliferate for 5 days, the number of viable cells was quantified by a tetrazolium-based colorimetric method as described by Pauwels *et al.*^{27,37}

Flow cell cytometry anti-CXCR4 antibody competition studies

Cell culture. Human leukaemia T cell lymphoblasts (Jurkat) were obtained from MRL (University of Hull, UK). These cells were cultured in RPMI 1640 medium treated with sterile filtered fetal bovine serum (FBS) (10%) and penicillin and streptomycin (100 units per

5 mL) antibiotics. The cells cultures were maintained at 37 °C in a humidified, CO₂ (5%) controlled atmosphere with subculturing done every 2–3 days as appropriate.

General procedure for binding assay with 12G-5 conjugated to phycoerythrin

Phycoerythrin (PE)-conjugated mouse monoclonal anti-human CXCR-4 and Mouse IgG2A isotype control-PE were purchased from R&D systems Europe, Abingdon, UK.

Cells are harvested at about 75% confluency, centrifuged, resuspended in 10 mL PBS and centrifuged again. Cells are kept on ice to prevent receptor internalisation. Cells are resuspended in 1.0 mL of PBS/0.25% BSA/0.01 M NaN₃ and viable cells are counted using trypan-blue exclusion test. Cells at a density of 1–2 × 10⁵ cells were aliquoted into polypropylene FACS tubes and preincubated with 20 μM of the compound (10 μL in 18.2 mΩ water) for one hour at 4 °C. A high concentration of compound was used to ensure saturation of the receptors. Thereafter, cells were washed with 1 mL of the buffer (PBS/0.25% BSA/0.01 M NaN₃) to remove the excess of compound that did not bind to the cells' receptors. Cells were then incubated with the 12G-5 mAb conjugated to phycoerythrin for a further 60 min. The cells were washed with 1 mL of the buffer and put in suspension in 300 μL of the buffer. Negative control was performed using the same protocol without the preincubation step. The binding of our compound was analysed by flow cytometry on a FACScan flow cytometer (BD Biosciences Europe, Erembodegem, Belgium) using the following FL channel FL-2 575/26 nm (PE/PI).

The potency of compounds is reported as a concentration required to inhibit a specified amount (%) of the mABs. The Mean Fluorescent Intensity (MFI) was used as a measure of binding and a quantitative way of calculating the inhibition percentage of mAb.

$$\% \text{ mAb inhibition} = 100 - \left(\left(\frac{(\text{MFI cells with compound} - \text{MFI negative control})}{(\text{MFI positive control} - \text{MFI negative control})} \right) \right)$$

Acknowledgements

Support was provided by the CNRS, the University of Burgundy and the Conseil Régional de Bourgogne through the 3MIM Project. S.P. and P.D. thank the Ministère de l'Enseignement Supérieur et de la Recherche for PhD grants. COST action TD 1007 PET-MRI is also

acknowledged for financing STSM of S.P. This work, in part, was supported by funding of the K.U. Leuven (GOA/10/014 and PF/10/018) and the Foundation of Scientific Research (FWO no. G.0485.08 and G.0528.12). Support was provided by Yorkshire Cancer Research (HEND376) and the University of Hull.

Notes and references

1. (a) M. Loetscher, T. Geiser, T. Oreilly, R. Zwahlen, M. Baggiolini and B. Moser, *J. Biol. Chem.*, 1994, **269**, 232 [CAS](#) ; (b) O. Jacobson and I. D. Weiss, *Theranostics*, 2013, **3**, 76 [CrossRef](#) [PubMed](#) ; (c) J. Kuil, T. Buckle and F. W. B. van Leeuwen, *Chem. Soc. Rev.*, 2012, **41**, 5239 [RSC](#) .
2. C. C. Bleul, M. Farzan, H. Choe, C. Parolin, I. Clark-Lewis, J. Sodroski and T. A. Springer, *Nature*, 1996, **382**, 829 [CrossRef](#) [CAS](#) [PubMed](#) .
3. W. T. Choi, S. Duggineni, Y. Xu, Z. Huang and J. An, *J. Med. Chem.*, 2012, **55**, 977 [CrossRef](#) [CAS](#) [PubMed](#) .
4. (a) A. P. Vicari and C. Caux, *Cytokine Growth Factor Rev.*, 2002, **13**, 143 [CrossRef](#) [CAS](#) ; (b) F. Balkwill, *Semin. Cancer Biol.*, 2004, **14**, 171 [CrossRef](#) [CAS](#) [PubMed](#) .
5. L. K. Gupta and V. Tripathi, *Int. J. Pharm. Pharm. Sci.*, 2012, **4**, 69 [CAS](#) .
6. (a) F. Baridaud, T. G. Edwards, M. Sharron, A. Brelot, N. Heveker, K. Price, F. Mortari, M. Alizon, M. Tsang and R. W. Doms, *J. Virol.*, 2001, **75**, 8957 [CrossRef](#) [PubMed](#) ; (b) B. Debnath, S. Xu, F. Grande, A. Garofalo and N. Neamati, *Theranostics*, 2013, **3**, 47 [CrossRef](#) [CAS](#) [PubMed](#) .
7. X. Liang and P. J. Sadler, *Chem. Soc. Rev.*, 2004, **33**, 246 [RSC](#) .
8. H. C. Joao, K. De Vreese, R. Pauwels, E. De Clercq, G. W. Henson and G. Bridger, *J. Med. Chem.*, 1995, **38**, 3865 [CrossRef](#) [CAS](#) .
9. L. O. Gerlach, R. T. Skerlj, G. J. Bridger and T. W. Schwartz, *J. Biol. Chem.*, 2001, **276**, 14153 [CAS](#) .
10. I. Kalatskaya, Y. A. Berchiche, S. Gravel, B. J. Limberg, J. S. Rosenbaum and N. Heveker, *Mol. Pharmacol.*, 2009, **75**, 1240 [CrossRef](#) [CAS](#) [PubMed](#) .
11. C. W. Hendrix, A. C. Collier, M. M. Lederman, D. Schols, R. B. Pollard, S. Brown, J. B. Jackson, R. W. Coombs, M. J. Glesby, C. W. Flexner, G. J. Bridger, K. Badel, R. T. MacFarland, G. W. Henson and G. Calandra, *J. Acquired Immune Defic. Syndr.*, 2004, **37**, 1253 [CrossRef](#) [CAS](#) .

12. (a) A. Cashen, S. Lopez, F. Gao, R. MacFarland, K. Badel and J. DiPersio, *Biol. Blood Marrow Transplant.*, 2008, **14**, 1253 [CrossRef](#) [CAS](#) [PubMed](#) ; (b) D. A. Stewart, C. Smith, R. MacFarland and G. Calandra, *Biol. Blood Marrow Transplant.*, 2009, **15**, 39 [CrossRef](#) [CAS](#) [PubMed](#) .
13. G. J. Bridger, R. T. Skerlj, D. Thornton, S. Padmanabhan, S. A. Martellucci, G. W. Henson, M. J. Abrams, N. Yamamoto, K. De Vreese, R. Pauwels and E. De Clercq, *J. Med. Chem.*, 1995, **38**, 266 [CrossRef](#) .
14. G. J. Bridger, R. T. Skerlj, S. Padmanabhan, S. A. Martellucci, G. W. Henson, S. Struyf, M. Witvrouw, D. Schols and E. De Clercq, *J. Med. Chem.*, 1999, **42**, 3971 [CrossRef](#) [CAS](#) [PubMed](#) .
15. T. M. Hunter, I. W. McNae, D. P. Simpson, A. M. Smith, S. Moggach, F. White, M. D. Walkinshaw, S. Parsons and P. J. Sadler, *Chem. – Eur. J.*, 2007, **13**, 40 [CrossRef](#) [PubMed](#) .
16. (a) G. C. Valks, G. McRobbie, E. A. Lewis, T. J. Hubin, T. M. Hunter, P. J. Sadler, C. Pannecouque, E. De Clercq and S. J. Archibald, *J. Med. Chem.*, 2006, **49**, 6162 [CrossRef](#) [CAS](#) [PubMed](#) ; (b) R. Smith, D. Huskens, D. Daelemans, R. E. Mewis, C. D. Garcia, A. N. Cain, T. N. Carder Freeman, C. Pannecouque, E. De Clercq, D. Schols and S. J. Archibald, *Dalton Trans.*, 2012, **41**, 11369 [RSC](#) ; (c) A. Khan, G. Nicholson, J. Greenman, L. Madden, G. McRobbie, C. Pannecouque, E. De Clercq, R. Ullom, D. L. Maples, R. L. Maples, J. D. Silversides, T. J. Hubin and S. J. Archibald, *J. Am. Chem. Soc.*, 2009, **131**, 3416–3417 [CrossRef](#) [CAS](#) [PubMed](#) .
17. (a) A. Aghanejad, A. R. Jalilian, Y. Fazaeli, D. Beiki, B. Fateh and A. Khalaj, *Radioanal. Nucl. Chem.*, 2014, **299**, 1635 [CrossRef](#) [CAS](#) ; (b) O. Jacobson, I. D. Weiss, L. Szajek, J. M. Farber and D. O. Kiesewetter, *Bioorg. Med. Chem.*, 2009, **17**, 1486 [CrossRef](#) [CAS](#) [PubMed](#) ; (c) S. Nimmagadda, M. Pullambhatla, K. Stone, G. Green, Z. M. Bhujwalla and M. G. Pomper, *Cancer Res.*, 2010, **70**, 3935 [CrossRef](#) [CAS](#) [PubMed](#) ; (d) A. Aghanejad, A. R. Jalilian, Y. Fazaeli, B. Alirezapoor, M. Pouladi, D. Beiki, S. Maus and A. Khalaj, *Sci. Pharm.*, 2014, **82**, 29 [CrossRef](#) [CAS](#) [PubMed](#) ; (e) S. V. Hartimath, U. M. Domanska, A. M. E. Walenkamp, R. A. J. O. Dierckx and E. F. J. de Vries, *Nucl. Med. Biol.*, 2013, **40**, 507 [CrossRef](#) [CAS](#) [PubMed](#) ; (f) J. C. Knight and F. R. Wuest, *MedChemComm*, 2012, **3**, 1039 [RSC](#) .
18. A. Khan, J. D. Silversides, L. Madden, J. Greenman and S. J. Archibald, *Chem. Commun.*, 2007, 416 [RSC](#) .

19. J. C. Knight, A. J. Hallett, A. Brancale, S. J. Paisey, R. W. E. Clarkson and P. G. Edwards, *ChemBioChem*, 2011, **12**, 2692 [CrossRef](#) [CAS](#) [PubMed](#) .
20. (a) M. Ciampolini, L. Fabbrizzi, A. Perotti, A. Poggi, B. Seghi and F. Zanobini, *Inorg. Chem.*, 1987, **26**, 3527 [CrossRef](#) [CAS](#) ; (b) G. J. Bridger, R. T. Skerlj, D. Thornton, S. Padmanabhan, S. A. Martellucci, G. W. Henson, M. J. Abrams, N. Yamamoto, K. De Vreese, R. Pauwels and E. De Clercq, *J. Med. Chem.*, 1995, **38**, 366 [CrossRef](#) [CAS](#) ; (c) D. Xu, P. G. Mattner, K. Prasad, O. Repic and T. J. Blacklock, *Tetrahedron Lett.*, 1996, **37**, 5301 [CrossRef](#) [CAS](#) ; (d) S. Brandes, C. Gros, F. Denat, P. Pullumbi and R. Guilard, *Bull. Soc. Chim. Fr.*, 1996, **133**, 65 [CAS](#) ; (e) D. Guillaume and G. R. Marshall, *Synth. Commun.*, 1998, **28**, 2903 [CrossRef](#) [CAS](#) ; (f) M. Le Baccon, F. Chuburu, L. Toupet, M. Soibinet, I. Dechamps-Olivier, J.-P. Barbier and M. Aplincourt, *New J. Chem.*, 2001, **25**, 1168 [RSC](#) ; (g) G. J. Bridger, S. Padmanabhan, R. T. Skerlj and D. M. Thornton, WO9312096A1, 1993 .
21. J. B. Baell, R. W. Gable, A. J. Harvey, N. Toovey, T. Herzog, W. Hansel and H. Wulff, *J. Med. Chem.*, 2004, **47**, 2326 [CrossRef](#) [CAS](#) [PubMed](#) .
22. L. O. Gerlach, J. S. Jakobsen, K. P. Jensen, M. R. Rosenkilde, R. T. Skerlj, U. Ryde, G. J. Bridger and T. W. Schwartz, *Biochemistry*, 2003, **42**, 710 [CrossRef](#) [CAS](#) [PubMed](#) .
23. R. M. Izatt, K. Pawlak and J. S. Bradshaw, *Chem. Rev.*, 1991, **91**, 1721 [CrossRef](#) [CAS](#) .
24. E. J. Billo, *Inorg. Chem.*, 1984, **23**, 236 [CrossRef](#) [CAS](#) .
25. P. S. Pallavicini, A. Perotti, A. Poggi, B. Seghi and L. Fabbrizzi, *J. Am. Chem. Soc.*, 1987, **109**, 5139 [CrossRef](#) [CAS](#) .
26. K. Princen, S. Haste, K. Vermeire, E. De Clercq and D. Schols, *Cytometry*, 2003, **51A**, 35 [CrossRef](#) [CAS](#) [PubMed](#) .
27. R. Pauwels, J. Balzarini, M. Baba, R. Snoeck, D. Schols, P. Herdewijn, J. Desmyter and E. De Clercq, *J. Virol. Methods*, 1988, **20**, 309 [CrossRef](#) [CAS](#) .
28. (a) T. J. Wadas, E. H. Wong, G. R. Weisman and C. J. Anderson, *Curr. Pharm. Des.*, 2007, **13**, 3 [CrossRef](#) [CAS](#) ; (b) C. A. Boswell, X. Sun, W. Niu, G. R. Weisman, E. H. Wong, A. L. Rheingold and C. J. Anderson, *J. Med. Chem.*, 2004, **47**, 1465 [CrossRef](#) [CAS](#) [PubMed](#) .
29. (a) R. P. Haugland, *The Handbook. A guide to Fluorescent Probes and Labeling Technologies*, Molecular Probes Inc., Eugene, Oregon, 10th edn, 2005 [Search PubMed](#) ; (b) G. Ulrich, R. Ziessel and A. Harriman, *Angew. Chem., Int. Ed.*, 2008, **47**, 1184 [CrossRef](#) [CAS](#) [PubMed](#) .

30. (a) A. Coskun and E. U. Akkaya, *Tetrahedron Lett.*, 2004, **45**, 4947 [CrossRef](#) [CAS](#) [PubMed](#) ; (b) Z. Dost, S. Atilgan and E. U. Akkaya, *Tetrahedron Lett.*, 2006, **62**, 8484 [CrossRef](#) [CAS](#) [PubMed](#) .
31. S. L. Niu, C. Massif, G. Ulrich, R. Ziessel, P.-Y. Renard and A. Romieu, *Org. Biomol. Chem.*, 2011, **9**, 66 [CAS](#) .
32. C. Bernhard, C. Goze, Y. Rousselin and F. Denat, *Chem. Commun.*, 2010, **46**, 8267 [RSC](#) .
33. M. Bellier, G. Duportail and R. Baati, *Tetrahedron Lett.*, 2010, **51**, 1269 [CrossRef](#) [PubMed](#) .
34. A. Ojida, T. Sakamoto, M. A. Inoue, S. H. Fujishima, G. Lippens and I. Hamachi, *J. Am. Chem. Soc.*, 2009, **131**, 6543 [CrossRef](#) [CAS](#) [PubMed](#) .
35. (a) S. Purser, P. R. Moore, S. Swallow and V. Gouverneur, *Chem. Soc. Rev.*, 2008, **37**, 320 [RSC](#) ; (b) P. W. Miller, N. J. Long, R. Vilar and A. D. Gee, *Angew. Chem., Int. Ed.*, 2008, **47**, 8998 [CrossRef](#) [CAS](#) [PubMed](#) ; (c) F. Dolle, D. Roeda, B. Kuhnast and M.-C. Lasne, *Fluorine and Health*, 2008, 3 [CAS](#) .
36. (a) R. Ting, M. J. Adams, T. J. Ruth and D. M. Perrin, *J. Am. Chem. Soc.*, 2005, **127**, 13094 [CrossRef](#) [CAS](#) [PubMed](#) ; (b) B. P. Burke, G. S. Clemente and S. J. Archibald, *Contrast Media Mol. Imaging*, 2014 DOI:10.1002/cmimi.1615 , in press.
37. C. Pannecouque, D. Daelemans and E. De Clercq, *Nat. Protoc.*, 2008, **3**, 427 [CrossRef](#) [CAS](#) [PubMed](#) .

Footnote

† Electronic supplementary information (ESI) available: Spectra and analytical data for the compounds synthesised.
See DOI: [10.1039/c4dt02972k](https://doi.org/10.1039/c4dt02972k)